2023 IEEE International Conference on Robotics and Automation (ICRA 2023)
May 29 - June 2, 2023. London, UK

Experimental evaluation of a method for improving experiment design in robot identification

Stefanie A. Zimmermann[1], Martin Enqvist[1], Svante Gunnarsson[1], Stig Moberg[2], Mikael Norrlöf[2]

***Abstract*— The control system of industrial robots is often model-based, and the quality of the model of high importance. Therefore, a fast and easy-to-use process for finding the model parameters from a combination of prior knowledge and measurement data is required. It has been shown that the experiment design can be improved in terms of short experiment times and an accurate parameter estimate if the robot configurations for the identification experiments are selected carefully. Estimates of the information matrix can be generated based on simulations for a number of candidate configurations, and an optimization problem can be solved for finding the optimal configurations. This work shows that the proposed method for improved experiment design works with a real manipulator, i.e. it is demonstrated that the experiment time is reduced significantly and the accuracy of the parameter estimate can be maintained or reduced if experiments are conducted only in the optimal manipulator configurations. It is also shown that the model improvement is relevant for realizing accurate control. Finally, the experimental data reveals that, in order to further improve the model accuracy, a more advanced model structure is needed for taking into account the commonly present nonlinear transmission stiffness of the robotic joints.**

I. INTRODUCTION

Following the approach of model-based control, a highly accurate description of the robotic manipulator is crucial. Estimating parametric robot models from experiment data is challenging since the system must operate in closed-loop and since different types on nonlinearities occur in the dynamic equations. Phenomena such as friction, torque and resolver ripple, transmission backlash, and hysteresis can hardly be neglected, and the mechanical structure of the manipulator as well as the transmission behavior are elastic. General challenges in robot identification are, e.g. , summarized in [1]. Because of these challenges, identification from data requires well-designed experiments and the choice of input signal during the data acquisition is a significant factor for the result of the parameter estimation, see e.g. [2]. Experiment design often relates to maximizing the information that is gained from the experiment while considering physical constraints, such as position, speed and torque limitations. Many aspects of input design for general linear time-invariant systems are well-understood. See e.g. [3] for an early reference and [4] for a more recent overview. However, experiment design for nonlinear systems is not yet fully theoretically explored, and most literature is about specific sub-classes of nonlinear systems, such as finite-impulse-response-type systems (see e.g. [5]) or nonlinear models that are composed of a known linear dynamic system interconnected with unknown static nonlinearities (see e.g. [6]).

Optimal experiment design in robotics has been studied already since the late 90s. Most methods parametrize the excitation as a Fourier series in order to find an optimal excitation trajectory. The method for optimizing the excitation trajectory that is presented in [7] aims directly at estimating the robot model parameters with minimal uncertainty, while an information matrix is maximized in [8] for guaranteeing a rich data set. A similar optimality criterion for finding a persistently exciting trajectory is chosen in [9] and the optimal trajectory is computed by using a memetic algorithm.

Using an identification approach in frequency domain, linearization of the dynamic equations around an operating point is needed, such that the frequency response functions (FRFs) can be estimated. Two aspects are therefore of particular interest in the experiment design: First, optimal linearization points (called robot *configurations*) for collecting informative data, and second, optimal excitation for best possible quality of the FRF estimate. This work is about finding the best robot configurations for data acquisition. It is assumed that a suitable excitation signal for FRF estimation is known and that it is not part of the experiment design problem. See e.g. [1], [10] and [11] for approaches on optimal input signals for FRF estimation. The idea of finding optimal manipulator configurations for parameter identification has mostly been treated related to robot calibration, which only involves static experiments. The goal is to minimize the TCP position error by identifying the geometric parameters and by estimating a static stiffness compensation. In order to find optimal robot configurations w.r.t. kinematic performance methods based on Jacobians of the robot's generalized coordinates are most common, see e.g. [12], [13]. An optimal compliance error compensation is derived in [14] by minimizing the covariance matrix, and a method for simultaneously identifying geometric and elasticity parameters is presented in [15]. Compared to robot calibration, this work aims to improve experiment design for the identification of a dynamic robot model.

A method for improved experiment design for frequency-domain identification was introduced in [16] and developed further in [17]. The proposed method finds the best combination of robot configurations from a set of candidates and is based on the information content of each candidate. While the information matrix is derived from noise assumptions in [16], simulations are used in [17] for deriving a more realistic estimate of the uncertainty of the system's FRFs. It

[1]Authors are with Faculty of Electrical Engineering, Linköping University, Sweden stefanie.zimmermann@liu.se
[2]Authors are with ABB Robotics, Västerås, Sweden stig.moberg@se.abb.com

has been shown in [17] that a realistic estimate of the FRFs' uncertainty is crucial for successful experiment design. Furthermore, the potential of improving the experiment design by the proposed method has been demonstrated with help of a simulation study. This paper completes the previous work by an experimental validation with a medium size industrial robot. It is shown that the experiment design is improved by the method in terms of efficiency and parameter accuracy. A significantly shorter time is needed for conducting data collection experiments and the average standard deviation of the parameter estimate is reduced.

The paper is structured as follows: Sec. II describes the model structure to be identified with the method sketched in Sec. III. The method for choosing robot configurations is described in Sec. IV, and results of a simulation-based design are given. Sec. V presents an experimental validation of the method for improving experiment design. Applying the method reveals the need for a model structure with a nonlinear function for the transmission stiffness, as outlined in Sec. VI. Conclusions are given in Sec. VII.

II. NONLINEAR GRAY-BOX ROBOT MODEL

The model structure that is used in this paper origins from [18], where a rigid body robot model with 6 degrees of freedom (DOFs) is extended by flexibility and friction in the joints. The transmission stiffness is modeled by spring-damper pairs, acting in the direction of rotation of the joint. In addition to the 6 spring-damper pairs describing the transmission flexibility, joints 1 to 3 are modeled with two more spring-damper pairs that take into account bearing and structural flexibility. The vector of joint angles is named q_a or q_m depending if it is expressed on the arm or the motor side of the gearbox. A realization of q_a is called *configuration* of the robot. The angular motion between the rigid bodies due to elastic effects that act perpendicular to the direction of transmission is described by the variables q_e. The model dynamics can be expressed by the following set of differential equations:

$$\begin{aligned} M_m\ddot{q}_m + \tau_{fm} + r_g\tau_g &= \tau \\ M_{ae}\begin{bmatrix}\ddot{q}_a\\ \ddot{q}_e\end{bmatrix} + c_{ae} + g_{ae} &= \begin{bmatrix}\tau_g\\ \tau_e\end{bmatrix} \\ k_g\cdot(r_g q_m - q_a) + d_g\cdot(r_g\dot{q}_m - \dot{q}_a) &= \tau_g \\ -k_e q_e - d_e\dot{q}_e &= \tau_e \end{aligned} \tag{1}$$

where $M_m = \mathrm{diag}(J_{m1},...,J_{m6})$ is the matrix of motor inertias, $\tau_{fm} = \tau_{fm}(\dot{q}_m)$ is the motor friction, r_g is the matrix of inverse gear ratios, $M_{ae} = M(q_a, q_e)$ is the inertia matrix, $c_{ae} = c(q_a, q_e, \dot{q}_a, \dot{q}_e)$ is the velocity dependent torque, $g_{ae} = g(q_a, q_e)$ is the gravity torque, k_g, k_e, d_g and d_e are the joint stiffness and damping constants in the direction of transmission (index g) and perpendicular to the direction of transmission (index e). Choosing the state vector $x = [q_m, q_a, q_e, \dot{q}_m, \dot{q}_a, \dot{q}_e]^T$ and the applied torque $\tau = u$ as input results in a state space model, containing $\dim(q_m) + \dim(q_e)$ stiffness parameters that shall be estimated from data. Modeling approaches with many more DOFs that take into account distributed link flexibility and more advanced joint models have been implemented successfully, see e.g. [19]. Nevertheless, lumped parameter models such as (1) are most common for control purposes. A schematic drawing is shown in Fig. 1.

In the scope of this work, the mass and inertia parameters are assumed to be known, while the friction parameters are identified from experimental data in a pre-step to the actual identification as explained in Sec. III. Since some parameters are assumed to be known prior to the identification, the model is called a gray-box model.

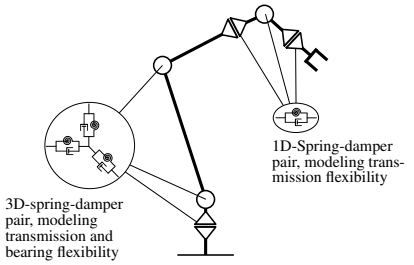

Fig. 1. Gray-box model of an 6-axis manipulator.

III. PARAMETER IDENTIFICATION IN FREQUENCY-DOMAIN

The overall goal is to identify the stiffness (and damping) parameters of a nonlinear robot model (1), which are collected in the vector θ. From a control perspective it is most important to identify the resonance frequencies. This work therefore reduces the parameter set to stiffness constants only. A frequency-domain method is used which was proposed in [20] and described in more detail in [21]. The method is based on the assumption that the excitation signal is a small perturbation around a robot configuration, allowing linearization of (1) and the use of linear theory. The optimal parameters $\hat{\theta}$ are obtained by minimizing the weighted logarithmic error between the FRFs $\hat{G}^{(i)}(\omega)$ estimated from measurements and the parametric FRFs $G^{(i)}(\omega,\theta)$ of the linearized gray-box model:

$$\hat{\theta} = \arg\min_{\theta} \mathcal{F}(\omega,\theta) \tag{2}$$

$$\begin{aligned} \mathcal{F}(\omega,\theta) &= \sum_{i\in Q_c}\sum_{l=1}^{N_f}\left[\mathcal{E}^{(i)}(\omega_l,\theta)\right]^T W^{(i)}(\omega_l)\,\mathcal{E}^{(i)}(\omega_l,\theta) \\ \mathcal{E}^{(i)}(\omega_l,\theta) &= \log\mathrm{vec}(\hat{G}^{(i)}(\omega_l)) - \log\mathrm{vec}(G^{(i)}(\omega_l,\theta)) \end{aligned} \tag{3}$$

where $W^{(i)}(\omega)$ is a weighting matrix, and N_f the number of frequencies. $W^{(i)}(\omega)$ can be designed such that the frequency range of interest (e.g. around the (anti-)resonances) is weighted higher, or such that the diagonal elements of $G^{(i)}$ are prioritized. Note that the parameters in (2) are unconstrained. This can useful since a stiffness parameter that converges to a unrealistically high value can be assumed to be unnecessary and can be removed from θ. The logarithmic least squares criterion is used because of the large dynamic range of the highly resonant robot system. This criterion has improved numerical stability as well as robustness with

respect to outliers in the measurement data [22, p. 208 f.]. From a theoretical perspective, this criterion is not optimal since it gives inconsistent estimates. In practice, this is of minor importance since a good signal-to-noise ratio can be ensured.

For estimating the 6×6 FRFs $\hat{G}^{(i)}$ from motor torque to motor acceleration, only the built-in sensors of an industrial robot are used: Sensors measuring the current i_m of each motor, and resolvers, measuring the angular position q_m of the six actuators. Since the robot system is unstable, experiments need to be conducted in closed loop (see Fig. 2). This yields the challenge that the measured FRFs get biased due to the correlation between the input u and the additive noise v. For multivariable nonparametric FRF estimation, the orthogonal random phase multisine has been suggested as excitation signal [23], given certain amplitude constraints. Thus, all six motors are excited with a speed reference signal. The motor torque τ_m is recorded, which is derived from the current measurement i_m. A simple linear relation between i_m and τ_m is used under the assumption that the motor dynamics are much faster compared to the dynamics of the robot arm. In order to improve the quality of the FRF estimate $\hat{G}^{(i)}$, the effect of disturbances and nonlinear effects must be dealt with. Therefore, and for calculating the uncertainty $\Lambda_{\hat{G}}^{(i)}$ of the FRF estimate, multiple periods are measured and additional experiments are performed in each robot configuration. Logarithmic averaging is then used for estimating $\hat{G}^{(i)}$ [24]. Averaging over multiple periods reduces random noise, whereas averaging over different experiments also reduces the effect of nonlinearities, since different realizations of the random phase multi-sine input signal are used [25].

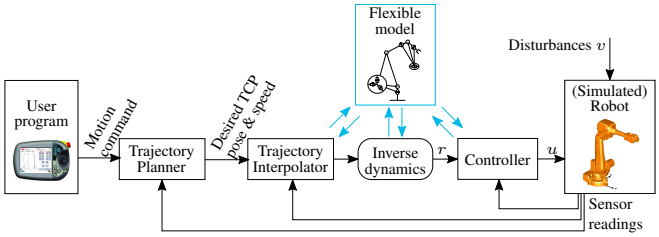

Fig. 2. Control framework of an industrial robot.

IV. EXPERIMENT DESIGN

A. The method

The goal is to improve the experiment design such that the time that is needed for conducting the identification experiments is reduced, and the identification accuracy is increased. Since the information content about the parameters θ differs between different configurations, experiments should be performed in the most informative configurations w. r. t. θ. A method for selecting the best manipulator configurations from a set of candidates was proposed in [16] and adapted by [17]. Based on the information matrix H_i, a convex optimization problem w.r.t. λ is formulated:

$$\begin{aligned} &\text{minimize} && \log\det\left[\sum\nolimits_{i\in Q_c} \lambda_i H_i\right]^{-1} \\ &\text{subject to} && \lambda \geq 0, \;\; 1^T\lambda = 1 \end{aligned} \tag{4}$$

where the set of candidate configurations Q_c must be chosen such that it covers the workspace of the manipulator. Then, the information matrix is computed for each candidate:

$$H_i = 2Re\left\{\overline{\Psi^{(i)}(\theta_0)}\left[\Lambda_0^{(i)}\right]^{-1}\left[\Psi^{(i)}(\theta_0)\right]^T\right\} \tag{5}$$

where $\left[\Psi^{(i)}(\theta_0)\right]^T = \frac{\partial G^{(i)}(\theta_0)}{\partial\theta}$ is the Jacobian of the parametric model FRFs $G^{(i)}(\theta_0)$ w.r.t. the parameters θ and is computed using the central differences. θ_0 are the nominal parameters, which can, e.g., be obtained by identification based on data from a few experiments in random configurations. Another approach is described in [19], which allows to accurately model the manipulator without experiments based on catalog data of the components and the Finite Element Model of the structure. $\Lambda_0^{(i)}$ is the total variance matrix of the FRF estimate:

$$\Lambda_0^{(i)} = \text{diag}\left[W^{(i)}\Lambda_{\hat{G}}^{(i)}(\omega_1), \ldots, W^{(i)}\Lambda_{\hat{G}}^{(i)}(\omega_{N_f})\right] \tag{6}$$

where $W^{(i)}(\omega)$ is a weighting matrix. Multiple experiments are simulated in each configuration $i \in Q_c$ for estimating $\hat{G}^{(i)}$ and for computing the block-diagonal matrix $\Lambda_0^{(i)}$ from the FRF uncertainties $\Lambda_{\hat{G}}^{(i)}$. This might be costly but the effort can be motivated since the resulting experiment design is used for the identification of all robots of the same type. Once the optimal configurations are found, only few experiments need to be conducted with the real robot for identifying different robot individuals. That is, non-parametric FRFs $\hat{G}^{(i)}$ need to be estimated only for the optimal configurations Q_{opt}. Compared to this approach of gaining $\Lambda_0^{(i)}$ from simulated data, [16] suggest to express the FRF estimates as the sum of the parametric FRF and a zero mean measurement noise. This allows to determine the variance matrix simply from the power spectra of the noise and the reference signal. The drawback of this approach is that $\Lambda_0^{(i)}$ does not relate to the system's nonlinearities. It is shown in [17] that a realistic estimate of $\Lambda_0^{(i)}$ that is gained from simulations is crucial for successful experiment design and that the approach of assumed noise may give worse results.

B. Simulation-based experiment design

The model to be identified contains linear functions for describing the transmission stiffness, i.e. $\theta = [\theta_1, \ldots, \theta_{12}]$ contains 12 stiffness parameters (three 3-D + three 1-D joints). For estimating the uncertainty of the FRF estimate $\Lambda_0^{(i)}$, simulations are performed in [17] with a very realistic manipulator model that describes the gear transmission as a damped stiffening spring and that includes other deterministic nonlinearities such as motor torque ripple and resolver position error. This is called "Case II" in [17]. Using another simulation set-up with a simpler robot that has linear transmission characteristics and that does not consider the previously named nonlinearities is called "Case I". Just as the real robot, the simulated robot is mounted on the floor and the maximum payload is attached at the end-effector. Data is generated by simulation as described in Sec. III and the motor torques and accelerations of all axes are recorded.

300 candidate configurations Q_c are arbitrarily chosen such that they are spread out in the robot's workspace.
Based on the two simulated robots as well as the nominal model, the problem (4) is solved and two sets $Q_{opt,I}$ and $Q_{opt,II}$ are found. Both sets contain 7 manipulator configurations each that are optimal among the 300 candidates. The simulation study presented in [17] shows that the experiment design is improved by the method. Using data that was collected in the configurations Q_{opt}, the experiment time can be reduced significantly compared to collecting estimation data in 300 random configurations, and the accuracy of the parameter estimate is increased both in terms of average standard deviation and bias. In the following, it will be shown that the results hold for measurement data recorded on a real manipulator, and also that the identified model is relevant for realizing accurate control.

V. Experimental results and model validation

A. Framework

A robot model as (1) is identified, i.e. 12 stiffness parameters are estimated from data. The damping and friction parameters are assumed to be known from separate measurements. Experiments as described in Sec. III are conducted with a medium size industrial robot together with a control framework as shown in Fig. 2. A joint trajectory is generated from the user input and transformed into a corresponding motor trajectory with the help of the dynamic flexible robot model (1). The robot controller contains both feedback and feedforward architecture: The feedforward controller uses the known trajectory and an inverse dynamics model for generating a computed torque [26], while the feedback controller handles the non-zero tracking error, which occurs due to model errors and disturbances.

B. Estimation data

For accurately estimating the FRF in a certain configuration, a minimum number of experiments is required [21]. Similarly as described in [27], 4 different realizations of the input signal are applied 6 times (orthogonal phases), giving 24 experiments in each configuration. Thus, equally many data is recorded in each of 49 robot configurations Q_{49}.
Among the 49 test configurations, 21 are randomly chosen such that they are distributed over the workspace of the manipulator (Q_{rem}). Furthermore, Q_{49} contains several sub-sets with 7 configurations each, see Table I. $Q_{opt,I}$ and $Q_{opt,II}$ are the optimal configurations according to the results of (4) found in [17] (see Sec. IV-B), Q_{mirr} are the configurations of $Q_{opt,II}$ but mirrored at the manipulators vertical-front plane, Q_{low,τ_2} are the 7 configurations of Q_{49} with lowest gravity torque on axis 2, and Q_{guess} are 7 configurations that a skilled engineer would intuitively choose for collecting data. The data sets Q_{rand} contain 7 configurations each that are randomly chosen from Q_{rem}.

C. Validation in frequency domain

The experimental design is considered to be improved if an appropriate compromise can be found between the following criteria:

TABLE I
NOMENCLATURE OF ESTIMATION DATA AND CORRESPONDING MODELS.

Model name	Estimation data	No. of configs	Comment
M_{49}	Q_{49}	49	Combination of rows below
$M_{opt,I}$	$Q_{opt,I}$	7	Optimal, simulation Case I
$M_{opt,II}$	$Q_{opt,II}$	7	Optimal, simulation Case II
M_{guess}	Q_{guess}	7	Engineer's intuitive guess
M_{mirr}	Q_{mirr}	7	Mirrored comp. to $Q_{opt,II}$
M_{low,τ_2}	Q_{low,τ_2}	7	Low gravity torque in axis 2
$M_{rand,a-d}$	$Q_{rand,a-d}$	7	Randomly chosen

- Fewer experiment configurations are used for collecting data, such that the total experiment time is reduced.
- The model's FRFs are closer to the measured FRFs, i.e. the cost $\mathcal{F}(\omega,\theta)$ (3) is reduced.
- The average and worst-case standard deviation (STD) of the parameters $\hat{\theta}$ is reduced (see Sec. V-D).

For validation, a second set of data is collected in the configurations Q_{49} with new realizations of the input signal. Furthermore, a payload with only 50 % of the maximum mass is attached to the robot, compared to full payload for collecting the estimation data. A cost function similar to (3) is used for rating the models' quality, where the FRFs $\hat{G}^{(i)}$ are estimated from the validation data and θ are the estimated parameters using different estimation data. Only the (weighted) logarithmic amplitude-error between the FRFs is considered.

Fig. 3 shows the model cost for all validation configurations. For each model, the configurations (x-axis) are sorted from lowest to highest cost value (y-axis). The two middle columns of Table II show the worst-case cost, as well as the average cost w.r.t. the validation data. As expected, the model M_{49} performs globally best, i.e. it has the lowest average and the lowest worst-case cost. This might be obvious since M_{49} is derived from the largest amount of estimation data. For fulfilling the goal of reduced experiment time, models that are based on data from only 7 configurations are preferred. The estimation of M_{49} requires 7 times more data, i.e. a 7 times longer experiment time. $M_{opt,II}$ can be considered to be the best model among those that are found from less estimation data since it finds the best compromise between average and worst-case cost. Only $M_{rand,d}$ has a slightly lower average cost than $M_{opt,II}$, but it has a higher cost in the worst configuration.

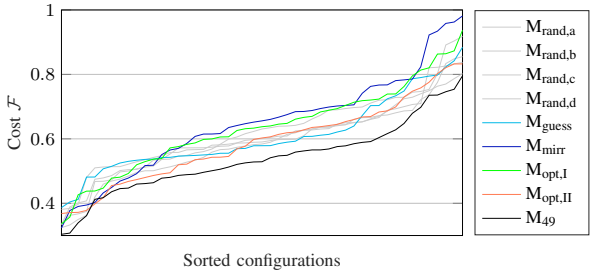

Fig. 3. Cost $\mathcal{F}$ of the identified models w.r.t. the validation data (weighted log-amplitude-error of the FRFs).

TABLE II

MODEL COST W.R.T. VALIDATION DATA FROM 49 CONFIGURATIONS AND AVERAGE STANDARD DEVIATION OF THE PARAMETERS IN θ.

Model	Worst-case cost	Average cost	Average STD θ
M_{49}	0.7956	0.5391	>10 %
$M_{opt,I}$	0.9369	0.6339	>10 %
$M_{opt,II}$	0.8326	0.5892	3.971 %
M_{guess}	0.8842	0.6074	4.826 %
M_{mirr}	0.9814	0.6477	>10 %
M_{low,τ_2}	1.0114	0.6135	>10 %
$M_{rand,a}$	0.8369	0.5979	>10 %
$M_{rand,b}$	0.9181	0.6208	8.496 %
$M_{rand,c}$	0.8024	0.6053	>10 %
$M_{rand,d}$	0.8552	0.5864	6.486 %

If visually analyzing the model FRF and the FRF estimated from data, a satisfying match is observed for many robot configurations. The model $M_{opt,II}$ matches the first eigenfrequency of the estimated FRF (Data) best of all models in the exemplary configuration 1, see Fig. 4(a) and (b). Note that Fig. 4 only shows two of the 6×6 FRFs in two exemplary configurations. Fig. 4(a), for example, shows the FRF from the torque of motor 2 to the acceleration of motor 2. In the second exemplary configuration (Fig. 4(c) and (d)), it can be observed that the eigenfrequencies of the measurement and those of all models except M_{low,τ_2} do not match accurately. This indicates that a model structure with linear transmission stiffness is not sufficient: In configuration 2, the low torque regions of axes 2 and 3 are excited and a lowered transmission stiffness would be needed to properly describe the system behavior (see also Sec. VI). This is validated by the fact that the model M_{low,τ_2} fits the measurement very well for configuration 2, but not for configuration 1. M_{low,τ_2} is a *local* model that is valid only for operation in regions with low gravity torque acting on axis 2. Thus, even though the model $M_{opt,II}$ is not optimally accurate in the entire robot workspace, it is the best compromise in terms of low model cost and reduced measurement time (see Table II).

D. Estimated model parameters and standard deviation

Fig. 5 shows the estimated model parameters and their standard deviations (STDs) obtained when solving (2). The model $M_{opt,II}$ has low STDs for all parameters, and the lowest average among the analyzed models (last column of Table II). Especially the STD of θ_6, which is a nonactuated stiffness parameter and therefore hard to identify, is significantly decreased by using the optimal configurations. Only M_{mirr} has a comparably low STD for θ_6, but θ_5 cannot be estimated with this experiment design set-up.

It can be observed that some parameter values differ a lot between the models, and that the STDs do not overlap. This indicates that the different models are *local* models for describing the system in the configurations of the estimation data set, but not in a global sense of the whole robot workspace. It can only be found models that are highly accurate for a few configurations (e.g. low torque in axis 2), or that are moderately accurate for many configurations (best compromise). It is likely that the model structure needs to be changed in order to find a global model representing the system in as many configurations as possible. As mentioned in Sec. V-C and as outlined in Sec. VI, it would be an improvement to formulate a nonlinear function for the transmission stiffness with weaker behavior for low motor torques.

Nevertheless, the experiment design has been improved, since the mean STD of the parameters is lowest for the model $M_{opt,II}$, and since the difficult parameter θ_6 can be identified accurately. The slightly increased cost $\mathcal{F}(\omega, \theta)$ compared to M_{49} can be accepted because only one seventh of the experiments are required for data collection.

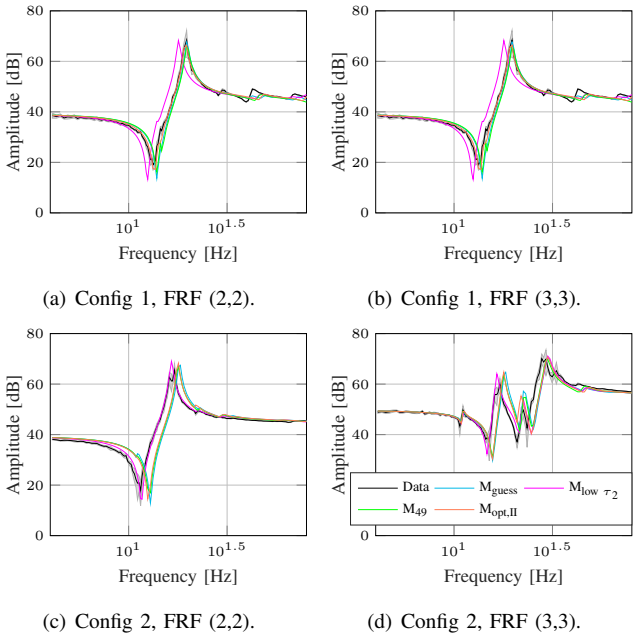

(a) Config 1, FRF (2,2). (b) Config 1, FRF (3,3).

(c) Config 2, FRF (2,2). (d) Config 2, FRF (3,3).

Fig. 4. Model FRFs end estimated FRFs from the torque of motor 2, 3 to the acceleration of motor 2, 3 in two exemplary configurations ("Data"). The uncertainty of the FRF estimate is shown as a gray region.

E. Validation in time domain and control performance

Since the primary use of the identified model is control, it is of interest to show that accurate control can be realized based on the identified parametric model. Since accurate TCP positioning is the desired outcome from a customer point of view, the absolute TCP position is used for validation.

Therefore, the robot is controlled using feedback and feedforward control based on the estimated model $M_{opt,II}$, and step-response experiments are done in random robot configurations. A very short movement with maximum acceleration of one axis at-the-time is chosen for validation, because this type of movement is known from experience to be most challenging in terms of path accuracy. The motor torques (currents) are measured with the built-in current sensors, and the absolute position of the TCP is traced with a Leica optical sensor. Fig. 6 shows the total TCP displacement due to a step movement of 1 deg in axis 1 (max. reached speed: 20 rad/s), starting from a robot configuration that is

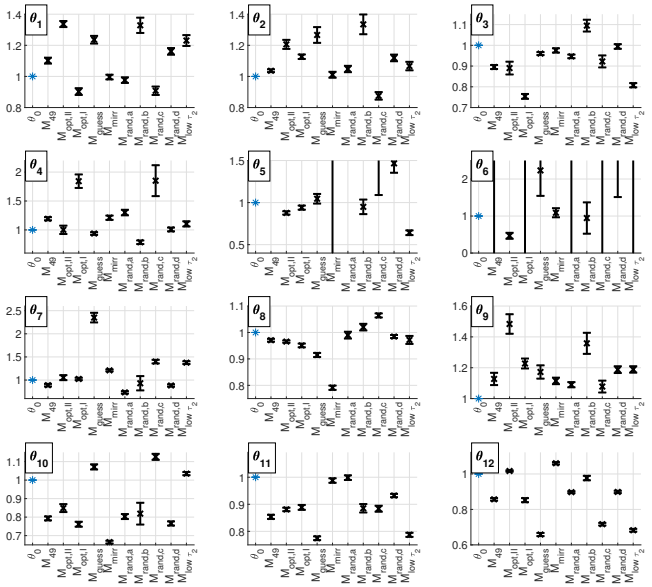

Fig. 5. Model parameters estimated with different data sets, normalized with initial parameters θ_0. Note that some values for θ_5 and θ_6 are outside the displayed range.

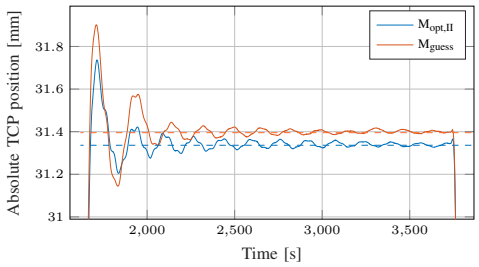

Fig. 6. Absolute TCP position if axis 1 is moved a step of 1 deg with maximum acceleration.

not part of the estimation data and that is assumed to be the worst-case configuration in terms of position accuracy. The control performance based on $M_{opt,II}$ and M_{guess} are compared w.r.t. the peak-to-peak oscillation of the final TCP position. Note that the steady-state difference in Fig. 6 is due to the position repeatability tolerance of the studied robot. It can be observed that the peak-to-peak oscillation is 0.46 mm if $M_{opt,II}$ is used compared to 0.53 mm with M_{guess}. Using the model $M_{opt,II}$ for control allows to ensure the guaranteed position accuracy of approximately 0.5 mm [28]. Based on the example presented, it can be concluded that the improvement of the model by optimal experiment design is relevant for high control performance.

VI. NEED FOR NONLINEAR TRANSMISSION MODEL

The gearbox torque is a function of the difference between arm angle and motor angle, which is nonlinear for commonly used robotic gears, see e.g. [29]. Here, the transmission stiffness is modeled as linear function (see Sec. II), leading to a model structure that cannot cover the system behavior globally. Manipulator models with stiffening springs in the main axes' transmission have been suggested and their potential has been demonstrated [21]. Unfortunately, it is not straightforward to estimate the parameters of such a model from the data set $Q_{opt,II}$, since the set was found with a linear transmission model. That is, the gradient $\Psi^{(i)}(\theta_0)$ in (5) only gives the sensitivity w.r.t. the linear stiffness parameters. It is therefore suggested for future work to adapt the experiment design problem formulation such that a manipulator model with nonlinear transmission stiffness can be handled. In that case, more parameters that describe the stiffness function would be added to θ and the equations would need to be linearized in the operating point. By combination of experiments in different robot configurations it might be possible to identify the nonlinear stiffness function. It is expected that the set $Q_{opt,II}$ will then contain configurations that allow to estimate the stiffness parameters for the different regions of applied motor torque (e.g. two stiffness parameters, one for high and one for low transmission torques).

VII. CONCLUSIONS AND FUTURE WORK

An optimization problem was solved for finding the best experiment configurations for the identification of stiffness parameters in frequency domain. The information matrices for each candidate configuration were estimated based on simulations, and 7 optimal manipulator configurations were found among 300 candidates. Based on experimental data from a real robot, this work validates the method and the resulting model. The experiment time can be reduced significantly and the accuracy of the parameter estimate can be increased, if experiments are done in the optimal configurations. Furthermore, it is shown that the model improvement due to optimized experiment design is relevant for the control design. The study also underlines that a model structure with linear transmission stiffness is inaccurate for certain applications, and that a more advanced parametrization is needed. Future work will therefore investigate the potential of nonlinear transmission models and the corresponding adaptations in the experiment design method. Another topic for future work is a combined optimization problem for finding optimal robot configurations and an optimal excitation signal in terms of low torque amplitudes. In this work, it was assumed that a suitable excitation signal for estimating the FRF is known, while future work could include the parametrized excitation signal in the optimization problem. For further decreasing the experiment time, different methods for the estimation of FRFs, such as local parametric methods [22, Ch. 12], will be considered.

ACKNOWLEDGMENT

This work was sponsored by the Vinnova competence center LINK-SIC.

REFERENCES

[1] F. Saupe and A. Knoblach, "Experimental determination of frequency response function estimates for flexible joint industrial manipulators with serial kinematics," *Mechanical Systems and Signal Processing*, vol. 52-53, pp. 60–72, 2015.

[2] L. Ljung, *System identification: Theory for the user*, 2nd ed. Upper Saddle River, N.J.: Prentice Hall, 1999.

[3] G. C. Goodwin and R. L. Payne, *Dynamic system identification: Experiment design and data analysis*, ser. Mathematics in science and engineering. New York and London: Academic Press, 1977, vol. 136.

[4] X. Bombois, M. Gevers, R. Hildebrand, and G. Solari, "Optimal experiment design for open and closed-loop system identification," *Communications in Information and Systems*, vol. 11, no. 3, pp. 197–224, 2011.

[5] A. de Cock, M. Gevers, and J. Schoukens, "D-optimal input design for nonlinear FIR-type systems: A dispersion-based approach," *Automatica*, vol. 73, pp. 88–100, 2016.

[6] T. L. Vincent, C. Novara, K. Hsu, and K. Poolla, "Input design for structured nonlinear system identification," *Automatica*, vol. 46, no. 6, pp. 990–998, 2010.

[7] J. Swevers, C. Ganseman, D. B. Tukel, J. de Schutter, and H. van Brussel, "Optimal robot excitation and identification," *IEEE Transactions on Robotics and Automation*, vol. 13, no. 5, pp. 730–740, 1997.

[8] J. Vantilt, E. Aertbeliën, F. de Groote, and J. de Schutter, "Optimal excitation and identification of the dynamic model of robotic systems with compliant actuators," in *2015 IEEE International Conference on Robotics and Automation*, 2015, pp. 2117–2124.

[9] A. Tika, J. Ulmen, and N. Bajcinca, "Dynamic Parameter Estimation Utilizing Optimized Trajectories," in *2020 IEEE/RSJ International Conference on Intelligent Robots and Systems*. IEEE, 2020, pp. 7300–7307.

[10] B. Boukhebouz, G. Mercere, M. Grossard, X. Lamy, and E. Laroche, "Identification of single flexible-joint robot dynamics: a nonparametric approach," in *2020 28th Mediterranean Conference on Control and Automation (MED)*. IEEE, 2020, pp. 357–362.

[11] N. Dirkx, M. Bosselaar, and T. Oomen, "Peak Amplitude-Constrained Experiment Design for FRF Identification of MIMO Motion Systems," in *2022 IEEE 17th International Conference on Advanced Motion Control*. IEEE, 2022, pp. 256–261.

[12] M. Hu, H. Wang, and X. Pan, "Optimal configuration selection for stiffness identification of 7-Dof collaborative robots," *Intelligent Service Robotics*, vol. 13, no. 3, pp. 379–391, 2020.

[13] C. Dumas, S. Caro, M. Cherif, S. Garnier, and B. Furet, "Joint stiffness identification of industrial serial robots," *Robotica*, vol. 30, no. 4, pp. 649–659, 2012.

[14] Y. Wu, A. Klimchik, A. Pashkevich, S. Caro, and B. Furet, "Optimality Criteria for Measurement Poses Selection in Calibration of Robot Stiffness Parameters," in *Proceedings of the ASME 11th biennial conference on engineering systems design and analysis 2012*. New York: ASME, 2012, pp. 185–194.

[15] S. Gadringer, P. Klement, H. Gattringer, A. Mueller, and R. Naderer, "Simultaneous Calibration and Stiffness Identification of Flexible Link Robots Using Lumped Parameter Model," in *Advances in Service and Industrial Robotics*, ser. Mechanisms and Machine Science, A. Müller and M. Brandstötter, Eds. Cham: Springer International Publishing, 2022, vol. 120, pp. 52–59.

[16] E. Wernholt and J. Löfberg, "Experiment design for identification of nonlinear gray-box models with application to industrial robots," in *46th IEEE Conference on Decision and Control*. Piscataway, N.J.: Institute of Electrical and Electronics Engineers, 2007, pp. 5110–5116.

[17] S. A. Zimmermann, M. Enqvist, S. Gunnarsson, S. Moberg, and M. Norrlöf, "Improving experiment design for frequency-domain identification of industrial robots," in *2nd Modeling, Estimation and Control Conference (MECC)*. IFAC-PapersOnLine, 2022.

[18] J. Öhr, S. Moberg, E. Wernholt, S. Hanssen, J. Pettersson, S. Persson, and S. Sander-Tavallaey, "Identification of flexibility parameters of 6-axis industrial manipulator models," *Proceedings of International Conference on Noise and Vibration Engineering*, vol. 6, 2006.

[19] S. A. Zimmermann, T. F. C. Berninger, J. Derkx, and D. J. Rixen, "Dynamic modeling of robotic manipulators for accuracy evaluation," in *2020 IEEE International Conference on Robotics and Automation (ICRA)*. Piscataway, NJ: IEEE, 2020, pp. 8144–8150.

[20] E. Wernholt and S. Moberg, "Frequency-Domain Gray-Box Identification of Industrial Robots," *IFAC Proceedings Volumes*, vol. 41, no. 2, pp. 15 372–15 380, 2008.

[21] S. Moberg, E. Wernholt, S. Hanssen, and T. Brogårdh, "Modeling and Parameter Estimation of Robot Manipulators Using Extended Flexible Joint Models," *Journal of Dynamic Systems, Measurement, and Control*, vol. 136, no. 3, 2014.

[22] R. Pintelon and J. Schoukens, *System identification: A frequency domain approach*, 2nd ed. Hoboken, N.J.: John Wiley & Sons Inc, 2012.

[23] T. Dobrowiecki and J. Schoukens, "Measuring a linear approximation to weakly nonlinear MIMO systems," *Automatica*, vol. 43, no. 10, pp. 1737–1751, 2007.

[24] P. Guillaume, "Frequency response measurements of multivariable systems using nonlinear averaging techniques," *IEEE Transactions on Instrumentation and Measurement*, vol. 47, no. 3, pp. 796–800, 1998.

[25] E. Wernholt and S. Gunnarsson, "Detection and Estimation of Nonlinear Distortions in Industrial Robots," in *2006 IEEE Instrumentation and Measurement Technology Conference Proceedings*. IEEE, 2006, pp. 1913–1918.

[26] M. W. Spong, S. Hutchinson, and M. a. Vidyasagar, *Robot Modeling and Control*, 2nd ed., 2020.

[27] E. Wernholt and S. Gunnarsson, "Estimation of Nonlinear Effects in Frequency Domain Identification of Industrial Robots," *IEEE Transactions on Instrumentation and Measurement*, vol. 57, no. 4, pp. 856–863, 2008.

[28] ABB Robotics, "Absolute Accuracy: Industrial robot option," 2010. [Online]. Available: https://library.e.abb.com/public/931fcb281dbe7fecc1257b1300579a6a/AbsAccPR10072EN_R5.pdf

[29] W. Seyfferth, A. J. Maghzal, and J. Angeles, "Nonlinear modeling and parameter identification of harmonic drive robotic transmissions," in *Robotics and automation*, ser. 1050-4729. IEEE, 1995, pp. 3027–3032.